Proceedings of 12th Cambridge Workshop on Cool Stars, Stellar Systems, & The Sun, 2003 University of Colorado.

FUSE Observations of the Active K Dwarf AB Doradus

R.D. Robinson[1], T.B. Ake[1], A.K. Dupree[2], J.L. Linsky[3]

Abstract.

In this paper we report on flaring activity observed in high time resolution FUV observations of the active K dwarf star AB Doradus, taken with the FUSE satellite. These observations include data on the C III (λ1175) and O VI ($\lambda\lambda$1032,1037) lines as well as the FUV continuum. During 29 hours of observation, two large flares and >10 smaller events were observed. Here we describe the time history of these events as well as a search for unresolved microflaring activity.

1. Introduction

AB Doradus is an extremely active ZAMS or slightly PMS star with a spectral type of K0-2 IV–V. It has a rotational velocity of $\sim$ 100 km s^{-1} and a rotation period of only 12.4 hours, making it one of the most rapidly rotating, and therefore most magnetically active, of all nearby K stars. An active chromosphere, starspots, flares and prominences have all been observed (see, e.g. Collier Cameron et al. 1999; Donati et al. 1999; Vilhu et al. 1998). Its special importance is that because of its proximity (15 pc) it is bright enough for high time resolution and moderately high spectral resolution observations. For these reasons, it was chosen as an ERO target during the early part of the FUSE mission.

These observations were carried out on 1999 Oct 20, Oct 22 and Dec 14 for 6 hr, 11.5 hr and 11.4 hr respectively. In all cases the data were obtained using the TTAG operating mode, where the time and location of each photon is recorded. The star was observed through the 30"×30" aperture, giving a spectral resolution of 15,000. The large southern declination of the source allowed us to observe it continuously, except for gaps caused by passage through the SAA. Unfortunately, the telescope was not fully aligned during this time, so only the 978–1188 Å region was covered. This region, however, includes prominent lines of C III (λ1175) and O VI ($\lambda\lambda$1032,1037) as well as samples of the FUV continuum. We therefore have diagnostics for the photosphere/lower chromosphere (continuum), the chromosphere (C III) and the transition region/lower corona

[1]Dept of Physics and Astronomy-Johns Hopkins University/ Computer Sciences Corporation

[2]Harvard-Smithsonian Center for Astrophysics

[3]Joint Institute for Laboratory Astrophysics/ University of Colorado

(O VI), which are invaluable in investigating the physical processes occurring during a stellar flare.

A preliminary study of this data set has been presented by Ake et al. (2000), who studied the quiescent spectrum as well as some aspects of a large flare event occurring on 1999 Oct 22. In the present paper we concentrate on the temporal behavior of the observed flares.

2. Time Histories of the Larger Flares

Figure 1 shows the time variations for two large flare events seen during the program. On the left we show a flare seen during the 20 Oct visit. The critical aspect of this flare is that while the line enhancements are rather modest (factors of 8 and 5 for O VI and C III respectively) the continuum increases by a factor of >100. While the the continuum enhancement started about 30s **before** the line increases, it is possible that the initial line increases are simply below the threshold of detectability, since the main burst (occurring ∼1 minute into the flare) occurs simultaneously in the lines and continuum. The main difference between the behavior of the lines and continuum appears to occur during the decay phase, since the continuum decays much more rapidly than the lines, reaching the basal level about 6 minutes after the start of the flare, while the O VI lines maintain an enhanced level for almost an hour (see below).

The right hand side of figure 1 shows the time variations for a rather complex flare seen during the 22 Oct visit. In this flare the magnitude of the flux increases in the lines and continuum are roughly compatible and there is a significant difference in the details of the time histories. For example; (a) The flare starts simultaneously in C III and the continuum but is delayed by about 3 minutes in O VI (though there is a *slight* increase in O VI starting 1 minute into the flare). (b) The rise phase is gradual in C III and the continuum, lasting more than 3 minutes. The C III flux shows several short lived bursts during the rise phase which are not apparent in either the continuum or O VI. The event is also much more impulsive in O VI. (c) The flare peak observed in the continuum and O VI follows the peak in C III by 10s and 40s respectively. (d) An enhancement in the continuum starting at 8.5 minutes is not observed in either of the emission lines. This is consistent with the behavior seen in Flare 1, where the continuum enhancement was much larger than that of the lines.

3. Time Histories of Smaller Flare Events

In Figure 2 (right) we show the first half of the 22 Oct time sequence, displayed with a large binning factor to improve the S/N of each time step. In addition to the large flare event (Figure 1, right) starting at 210 minutes there are a large number of smaller bursts which have been marked. Note that these small flares are much more evident in the lines than the continuum, in some cases showing no continuum enhancement at all. The flares are also all relatively long duration, often lasting 5 minutes or more. This is in contrast to small flare events seen on dMe stars, which often last for only 10–20s (Robinson, Carpenter & Percival 1999). Finally, there is no strong evidence for impulsive phase activity in these

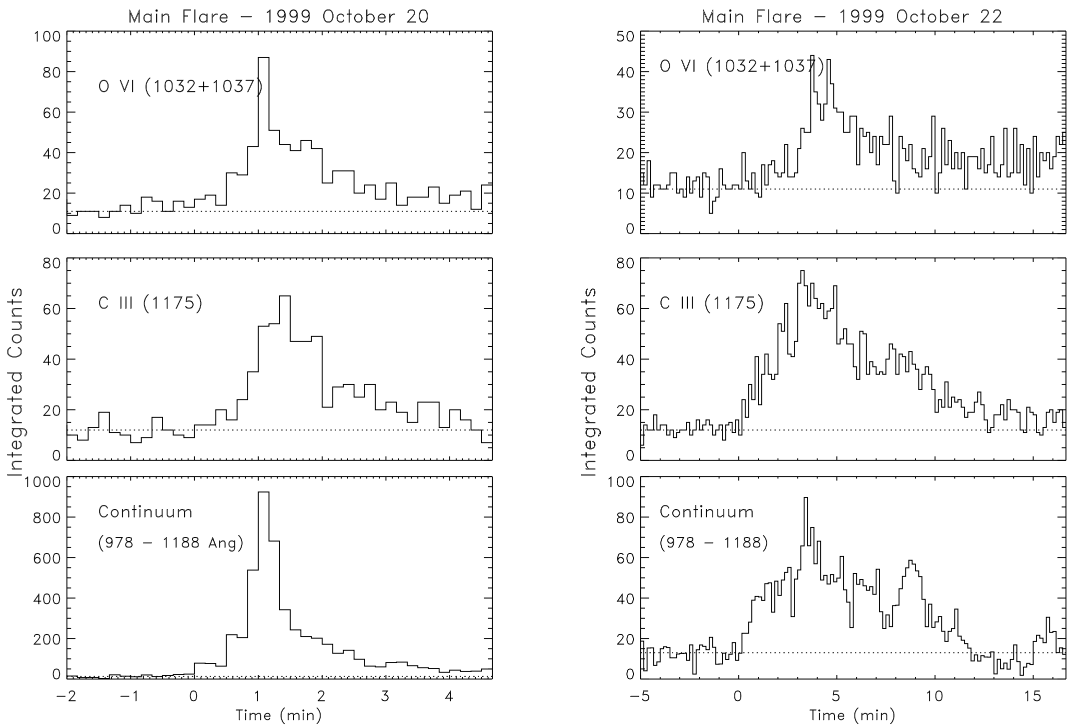

Figure 1. (Left) Time history of a large flare seen on 1999 Oct 20, as observed in the FUV continuum and several emission lines. The time sequences have been binned into 10s intervals . (Right) As above, except for a flare event on 1999 Oct 22.

bursts, even when viewed at a much higher time resolution. If the flares are actually groups of bursts, as seen in classical dMe flare stars (e.g. Robinson et al. 1995), then they must have long decay times and tend to merge.

4. The Decay Phase of Flares

Both of the large flare events in Figure 1 show enhanced emission following the impulsive phase of the burst. In both cases this emission is most pronounced in the hot O VI lines, where it lasts for 40-50 minutes following the end of the impulsive phase (e.g. Figure 2, right, at a time of 220 min). The cooler C III lines and continuum are less enhanced and shorter lived. In flare 1 (Figure 2, left) the C III enhancement lasted only 6 minutes and there was no reliable enhancement in the continuum. This decay phase may represent emission from post-flare loop systems and should be observable in X-rays.

During the decay phase the nature of the emission changes dramatically. Figure 3, for example, shows a dramatic increase in the O VI $\lambda 1032$ line relative

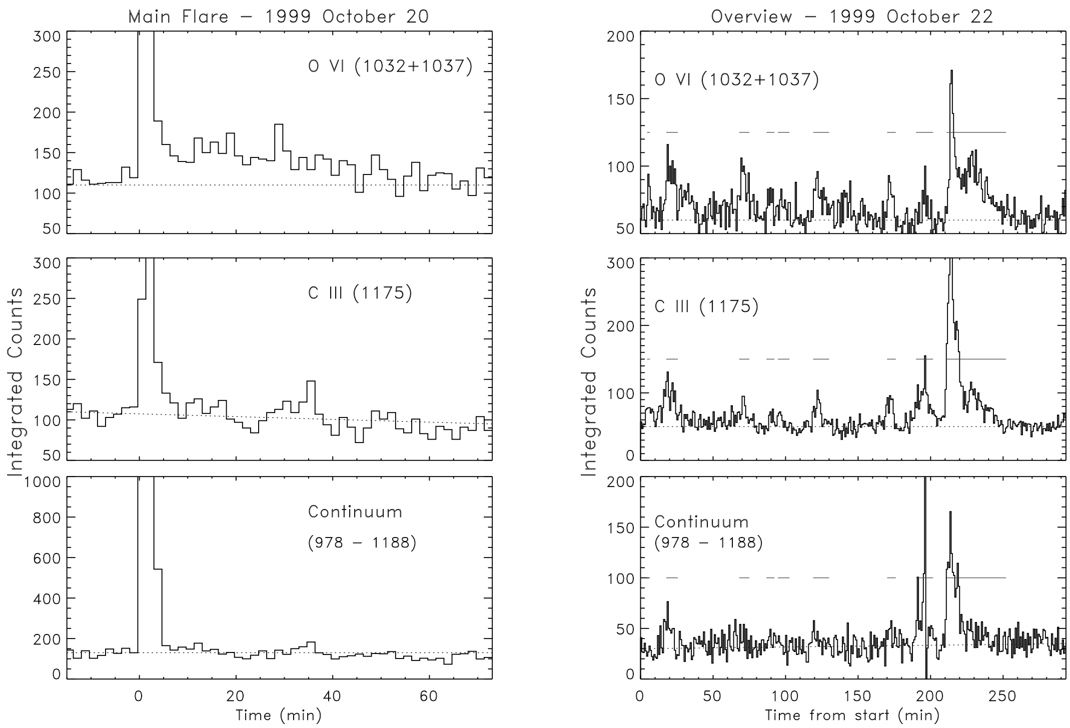

Figure 2. (Left) Time history of the main flare observed on 20 Oct, using 50s time bins to enhance the decay phase. (Right) The first half of the time sequence taken on 22 Oct, using time bins of 50s to enhance the signature of small flare events. Significant flare detections are marked. Note the decay phase of the flare starting at 210 minutes.

to the λ1037 line during the decay of the large 22 Oct flare. During the impulsive phase the line ratio equaled that seen in quiescence.

5. A Search for Microflares

Very weak flares will not be detectable as individual events in the time sequence. However, if there are enough of them they may affect the counting statistics of the noise and be detected. To search for these we first binned the line and continuum time sequences and obtained a histogram of the resultant counts per time interval. For low binning factors the noise dominates the microflare signal and you get a normal Poisson distribution. For higher binning factors the microflare signature becomes apparent as an excess in the high count range. The maximum signal occurs when the binning factor becomes comparable to the duration of the bursts.

A microflare search using the O VI lines is shown in Figure 4. A strong signal (representing $\sim$20% of the total count) is seen in the 20s binned data taken during 22 Oct. The signal is weaker in the 10s binned data , suggesting that the bursts have durations of 20s or more. Note that a similar analysis of the data taken on 14 Dec shows no evidence of microflare activity. This is consistent with the fact that the star was much more active in the earlier data set. While 12 individual flares were detected on 22 Oct, no flares were reliably detected in the Dec 14 data, though the observing times on the two dates were comparable.

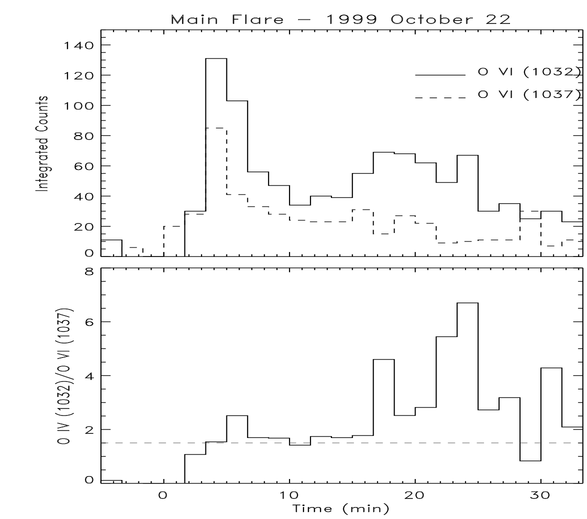

Figure 3. (Top) Time history of the fluxes in the O VI lines during the main flare seen on 22 Oct (Flare 2), using 150s time bins. The quiescent flux has been removed. (Bottom) Ratio of the O VI line fluxes during the flare. Note the dominance of the $\lambda1032$ line during the decay phase. The dashed line shows the line ratio in quiescence.

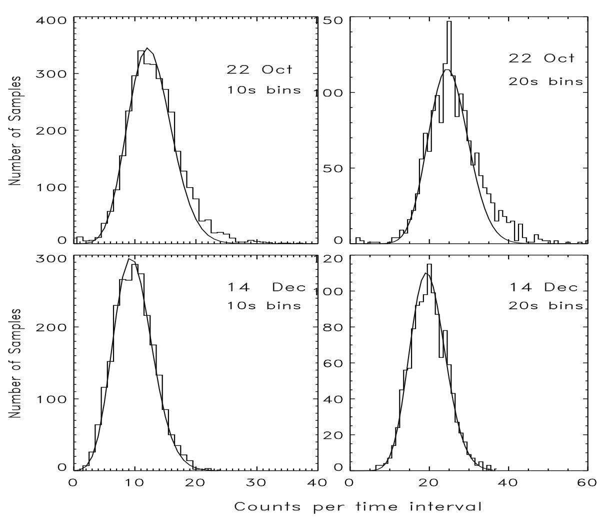

Figure 4. Histogram of observed counts in the O VI ($\lambda1032$ + $\lambda1037$) time sequence taken on 22 Oct (Top) and 14 Dec (Bottom). Time bins of 10s (Left) and 20s (Right) have been used. A Poisson distribution (blue line) which was fit to the peak and low count edge of the distribution is shown. Note the excess of high count bins in the 22 Oct data.

Acknowledgments. This work is based on data obtained for the Guaranteed Time Team by the NASA-CNES-CSA FUSE mission operated by the Johns Hopkins University. Financial support to U. S. participants has been provided by NASA contract NAS5-32985.

References

Ake, T.B., et al. 2000, ApJ, 538, L87

Collier Cameron, A., et al. 1999, MNRAS, 308, 493

Donati, J.F., Collier Cameron, A., Hussain, G.A.J., Semel, M. 1999, MNRAS, 302, 437

Robinson, R.D., Carpenter, K.G., Percival, J.W. & Bookbinder, J.A. 1995, ApJ, 451, 795

Robinson, R.D., Carpenter, K.G., & Percival, J.W. 1999, ApJ, 516, 916

Vilhu, O., et al. 1998, AJ, 115, 1610